

Research Article

Investigation and Simulation into the Effect of Shear, Concentrated and Distributed Loads on Solid Beam and Sandwich Beams with Different Core Material

¹Mohamed A.M. Shehata, ¹Ahmed S.A. Abou-Taleb and ²Ahmed Nassef

¹Mechanical Engineering Department, Faculty of Engineering, Fayoum University,

²Production Engineering and Mechanical Design Department, Faculty of Engineering, Port-Said University, Egypt

Abstract: Mechanical behaviors comparison of sandwich beams with diversified core material among epoxy, polyamide and wood, as well as, a solid steel beam was executed under a shear force, a concentrated load and a distributed load, with the attention that, the last two load types producing combined shear and bending stresses. Another mechanical behavior was considered where the static deflections from the specimens, especially the sandwich ones, have two contributor values provided from both bending and shear rigidities. A theoretical analysis and a numerical simulation were utilized for validation and comprehension purposes of the output results and conclusions. With taking into consideration, the comparison parameters that must be constant were the core thickness 10 mm, face thickness 3 mm, total thickness 16 mm, length 300 mm, width 20 mm and steel for faces material. The results conclude that employment of sandwich beam over a solid one with the same dimensions and vice versa, lead to a significant fluctuation in the object's mechanical behavior and weight, where the targeted result is high rigidity to weight ratio which provided by the sandwich beam. In other words, the specimen's flexural rigidity has a significant impact on its un-similar stresses' categories of shear stress, bending stress and these two stresses combined, as well as, its static deflection.

Keywords: Concentrated load, distributed load, flexural rigidity, sandwich beam, shear force, static deflection

INTRODUCTION

Researchers had their attention on the cumulative rising requirements of the market of multi-functionality, lighter weight, more capability to overcome combined loadings applied simultaneously and more reliable structures; therefore sandwich beams (laminated panels) were investigated, studied and presented as a solution to meet these requirements. The general basic principal utilized to obtain these more improved properties over the normal structures made from one material is repetitive layers structures, which leads to the design of the sandwich beams. As a result of this principle, different sandwich beams configurations were presented as normal basic cell sandwich beam has one core besides two faces sheets, hollow sandwich beams, sandwich beams with periodically variable cross-sections and sandwich beams with core has honeycomb shape in Romanoff and Varsta (2006); beside Hayes *et al.* (2004).

Due to the advantages of the sandwich structures as high stiffness, light-weight, high strength to toughness

ratio, heat-resisting and heat insulation; a vast scale of applications as sustainable energy, aerospace field, constructions work, biological components, transportation industry, thermo-mechanical products and fluid containing adoptive utilization of sandwich beams. Therefore, entirely comprehend about the mechanics of sandwich beams to fully use these advantages and functions to their fullest were the main objective of Noor *et al.* (1996), also Kim and Sawanson (2001).

At the modern days, Wang *et al.* (2000) reviewed and collected in their work the Euler-Bernoulli theory that neglects the shear effect and then the Timoshenko considers the shear effect and adds it to the linear beam theory. After Timoshenko by about twenty years, Reissner (1944) demonstrated the beginning of nonlinear plate theory with attention to the shear effect.

A sandwich beam structure was targeted to improve its shear mechanics through manufacturing and tying together fibre composite sandwich panels by glue, then adding them in specific flat-wise and edge-wise locations for constructions applications use. From

Corresponding Author: Mohamed A.M. Shehata, Mechanical Engineering Department, Faculty of Engineering, Fayoum University, Egypt, Tel.: +20 1004565665, +20 842150485

This work is licensed under a Creative Commons Attribution 4.0 International License (URL: <http://creativecommons.org/licenses/by/4.0/>).

observation by Manalo *et al.* (2013) at edgewise position, the performance of the glued sandwich beams is determined via the shear strength of the skin, while at the flat-wise position, the performance is limited by the shear strength of the core. After comparing the different types of results together, it is concluded that the skin at the edgewise location can take about 60% of the load, but on the other hand, at the flat-wise location it barely takes 20%.

Carrera (2003) presented a historical review about the classical broken line theory (zig-zag theory) for multi-layered structures, where the main objective about this theory is showing that transverse stresses are continuous at each layer interface. Besides, a comprehensive review of laminated composite plates and shells was done by Sayyad and Ghugal (2017) about varied fields as bending, buckling and free vibration. The authors focused on the shear deformable from different points of theories as a layerwise, zig-zag, single layer and exact elasticity solution, as well as, the use of finite element modeling.

Steeves and Fleck (2004) concentrated on introducing an indentation model with respect to elastic faces and an elastic-plastic core. It is concluded that sandwich beams with metallic faces and a metallic foam core is the equivalent to the best design possible of composite-polymer foam sandwich beams.

Specimens of sandwich structures were manufacturing and assembly from five components as two aluminum alloy face sheets and three cores via Jing *et al.* (2019). The cores configurations were designed as (i.e., the positive layered-gradient core, negative layered-gradient core and non-gradient monolithic core). The specimens were subjected to impact bending via utilization of drop-weight machine to provide various five impact energies as 9.80 J, 22.05 J, 39.19 J, 61.24 J and 88.18-J. From comparing the experimental results with the simulation (numerical) ones; it can observe that, when using low initial impact energy, all specimen classified under the global bending deformation without local cracks, but that is changeable under increased initial impact energy, the cracks will appear due to core tensile and shear. Also, it can conclude that the energy absorbing ratio with face sheets has increment relationship but with core has inverse one, where via increasing the impact energy, the energy absorbing ratio by face sheets increased, while the core's absorbing capability is decreasing.

The equations of equilibrium of nonlocal theories of the beams were derived by Reddy (2010). Besides, the derivation of controlling equilibrium equations of the first-order shear deformation and classical theories was executed. The author managed via using theoretical assumptions and finite element modeling to explain the effect on bending behavior from geometric non-linearity and non-local constitutive relationships.

In two articles of research, Magnucka-Blandzi (2011a, 2011b) studies the sandwich beams with metal

foam core from various static and dynamic performances via mathematical modeling and different hypotheses. The displacement of beam's flat cross section can be developed completely via using a generalization of the classical hypotheses, when, the basic concept of stationary total potential energy is considered; it is possible to create differential equations to describe the available system entirely.

To describe the type of beam, plate and shell characterized a single approximation of the displacements through the thickness was used by Abrate and di Sciuva (2017). From their work, it can be concluded that from three to five variables are sufficient to create sufficient models of these structures.

The present work is aiming to understand the impact of a shear force, a concentrated load and a distributed load on the mechanical behaviors of the solid beam and sandwich beams with a different core material. Bending stress, shear stress and a combination of these stresses, as well as, a static deflection are the main consequences on the specimens from the previously various loadings. The authors of the present work compare the theoretical results with its equivalent simulation ones to obtain a good agreement between them; and hence leading to verifications of the present work conclusions with other published work.

THEORETICAL ANALYSIS

First, the flexural rigidity was demonstrated because it is the pillar parameter for obtaining and analyzing the theoretical equations and results. Therefore, the shear stress, bending stress, combined shear and bending stresses; and static deflection were possibly obtainable via utilization the common factor between them, which is the flexural rigidity. The main assumptions of the utilized material involved in this analysis are behaving in a linear-elastic pattern, being isotropic and homogenous and fully bonding together without an occurrence of slipping or delamination. On the other hand, the used specimens varied between a solid beam and sandwich beam with different core material to fully understand the distinction between their mechanical behaviors. At the beginning of the analysis, the main components and dimensions of the sandwich specimen were necessary to presented in Fig. 1 to visualize the main parameters of the next theoretical equations.

Flexural rigidity of a sandwich beam: The achievement of flexural rigidity of symmetrical sandwich beam structured from three layers can be briefly summarized through Eq. (1-3). Eq. (1) presents the final form of neutral line offset c from the centroidal line of an unsymmetrical sandwich structure, which needed for further development. Eq. (2) shows the final form of bending moment M_b of cantilever sandwich

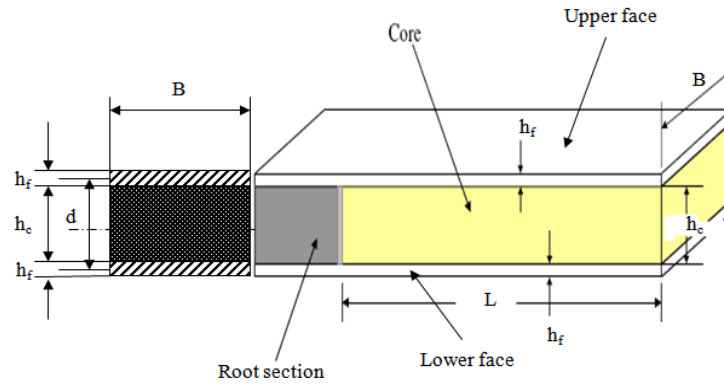


Fig. 1: Sandwich specimen's cross-sectional area, components and dimensions

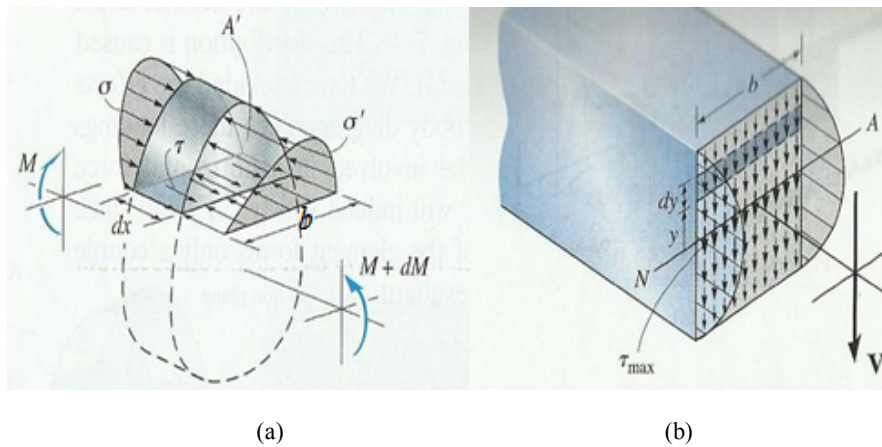


Fig. 2: Shear stress fluctuation showed: (a) on specimen's longitudinal orientation and (b) over specimen's cross-section

structure has a symmetrical cross-section, which utilized for complete development of targeted rigidity in Eq. (3). The flexural rigidity D is a significant parameter for its role of building the entire theoretical analysis around it. Note; the full details of complete derivation steps of the flexural rigidity of symmetrical or unsymmetrical cross-section of a three-layered sandwich beam was presented by the same authors of the present research in Shehata *et al.* (2019-accepted for publication):

$$c = \frac{E_{uf} h_{uf} \left(\frac{h_{uf} + h_c}{2} \right) - E_{lf} h_{lf} \left(\frac{h_{lf} + h_c}{2} \right)}{(E_{uf} h_{uf} + E_c h_c + E_{lf} h_{lf})} \quad (1)$$

In targeted case of a sandwich structure has a symmetrical cross-section, the following conditions will be applied ($E_{lf} = E_{uf} = E_f$ and $h_{lf} = h_{uf} = h_f$) to obtain Eq. (2), beside ($c = 0$ mm) to obtain Eq. (3):

$$M_b = \left(\frac{B}{R} \right) * \left[\frac{E_f}{3} \left[\left(c - \frac{h_c}{2} \right)^3 - \left(c - \frac{h_c}{2} - h_f \right)^3 \right] + E_c c^2 h_c + \frac{E_c h_c^3}{12} \right] \quad (2)$$

$$D = E_{eq} * I = M_b * R, \quad (3)$$

$$D = B * \left[\frac{E_f h_f^3}{6} + \frac{E_f h_f d^2}{2} + \frac{E_c h_c^3}{12} \right] = 2D_f + D_{fi} + D_{co}$$

Mass of sandwich beam: Nowadays, the sandwich beam has a large scale of spreading in different types of applications such as mechanical parts manufacturing, transportation industry, sustainable energy, civil engineering and communication instruments over the solid beam due to its advantage of high rigidity to weight ratio. Therefore the mass of symmetric sandwich beam has been comprehending from Fig. 1 and analyzed in a brief expression in Eq. (4):

$$m = m_f + m_c = (\rho_f * B * L * 2h_f) + (\rho_c * B * L * h_c), \quad (4)$$

$$m = BL * (2\rho_f h_f + \rho_c h_c).$$

Shear stress of symmetric sandwich beam: The shear stress of sandwich structure due to a shear force V will be analyzed with the utilization of previous sandwich beam dimensions in Fig. 1, shear stress fluctuation of the solid beam as a guiding sketch in Fig. 2 and flexural rigidity of symmetrical sandwich beam in Eq. (3).

Therefore, the transverse shear stress τ of symmetric sandwich beam composed of three layers

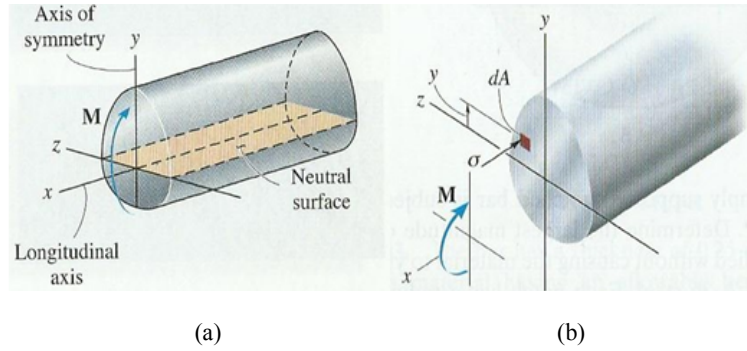


Fig. 3: Bending moment applied on: (a) cantilever specimen's cross-section as a whole and (b) specimen's specific element with showing the acted bending stress on it

can be generally described in Eq. (5), with knowing that longitudinal shear equals the transverse one; and also shear force $V = (dM/dx)$:

$$\tau = \int_y^{\frac{d}{2}} \frac{d\sigma}{dx} dy = \int_y^{\frac{d}{2}} \frac{dM}{dx} * \frac{y}{I} dy = \int_y^{\frac{d}{2}} \frac{dM}{dx} * \frac{E_f y}{D} dy, \quad (5)$$

$$\tau = \left(\frac{V}{D} \right) \int_y^{\frac{d}{2}} E_f y dy.$$

Based on Eq. (5), for the faces zones at $(h_c/2) < |y| \leq [(h_c/2) + h_f]$, the shear stress and strain can be expressed in Eq. (6) as follows:

$$\tau_f = \frac{V}{D} * \left[\int_y^{\frac{h_c}{2} + h_f} E_f y dy \right] \frac{V}{D} * \left[\frac{E_f}{2} * \left(\frac{h_c}{2} + h_f + y \right) * \left(\frac{h_c}{2} + h_f - y \right) \right] \quad (6)$$

,also: $\gamma_f = (\tau_f / G_f)$

With the same methodology, for the core zone at $|y| \leq (h_c/2)$ the shear stress and strain can be described in Eq. (7) as follows:

$$\tau_c = \frac{V}{D} * \left[\int_y^{\frac{h_c}{2}} E_c y dy + \int_{\frac{h_c}{2}}^{\frac{h_c}{2} + h_f} E_f y dy \right] = \frac{V}{D} * \left[\frac{E_c}{2} * \left(\frac{h_c^2}{4} - y^2 \right) + \frac{E_f h_f d}{2} \right] \quad (7)$$

,also: $\gamma_c = (\tau_c / G_c)$

At the outer surfaces of a sandwich beam, via substituting $|y| = (h_c/2) + h_f$ in Eq. (6) of faces zones, the shear stresses will have zero value at upper and lower surfaces.

The shear stress is continuous across the interfaces between face sheets and core, therefore by representing $y = h_c/2$ in Eq. (6) of faces zones or in Eq. (7) of the core zone, interfaces shear stress can be written in Eq. (8):

$$\tau_f \Big|_{y=\frac{h_c}{2}} = \tau_c \Big|_{y=\frac{h_c}{2}} = \frac{V}{D} * \left(\frac{E_f h_f d}{2} \right) \quad (8)$$

The maximum shear stress occurs at the neutral line of the entire sandwich beam, which can be obtained via substituting $y = 0$ in Eq. (7) of the core zone and then expressed in Eq. (9):

$$\tau_{\max} = \tau_c \Big|_{y=0} = \frac{V}{D} * \left(\frac{E_c h_c^2}{8} + \frac{E_f h_f d}{2} \right) \quad (9)$$

Bending stress of symmetric sandwich beam: The bending stress due to one of a bending moment M , a concentrated load F and a distributed load w will be analyzed using the previous sandwich beam dimensions in Fig. 1, the flexural rigidity of symmetrical sandwich beam in Eq. (3) and bending moment with its stress on solid beam utilized as instruction drawing in Fig. 3.

Therefore, the bending stress σ of symmetric sandwich beam composed of three layers can be generally described in Eq. (10) as:

$$\sigma = \frac{MEy}{R \int y dF} = \frac{MEy}{R \int y \sigma dA} = \frac{MEy}{R \int y \frac{E_f y}{R} B dy} = \frac{MEy}{B \int E_f y^2 dy} \quad (10)$$

Based on Eq. (10), for the faces zones at $(h_c/2) < |y| \leq [(h_c/2) + h_f]$, the bending stress and strain can be expressed in Eq. (11) as follows:

$$\sigma_{Bf} = \frac{ME_f y}{B * \left[\int_{-h_f}^{-\frac{h_c}{2}} E_f y^2 dy + \int_{\frac{h_c}{2}}^{\frac{h_c}{2} + h_f} E_c y^2 dy + \int_{\frac{h_c}{2}}^{\frac{h_c}{2} + h_f} E_f y^2 dy \right]}, \quad (11)$$

$$\sigma_{Bf} = \frac{ME_f y}{B * \left[\frac{E_f h_f^3}{6} + \frac{E_f h_f d^2}{2} + \frac{E_c h_c^3}{12} \right]},$$

$$\sigma_{Bf} = \frac{M * E_f y}{D} = \frac{FL * E_f y}{D} = \frac{wL^2 * E_f y}{D}.$$

,also: $\epsilon_{Bf} = (\sigma_{Bf} / E_f)$

With the same methodology, for the core zone at $|y| \leq (h_c/2)$, the bending stress and strain can be described in Eq. (12) as follows:

$$\sigma_{Bc} = \frac{ME_c y}{B * \left[\frac{E_f h_f^3}{6} + \frac{E_f h_f d^2}{2} + \frac{E_c h_c^3}{12} \right]}, \quad (12)$$

$$\sigma_{Bc} = \frac{M * E_c y}{D} = \frac{FL * E_c y}{D} = \frac{wL^2 * E_c y}{D}$$

,also: $\varepsilon_{Bc} = (\sigma_{Bc} / E_c)$

At the outer upper and lower surfaces of the sandwich beam, via substituting the thickness y in Eq. (11) with its maximum value and with its tension and compression sign, respectively, maximum bending stresses will be obtainable at both tension and compression directions.

To obtain the bending stress across the interfaces between the core and face sheets within a simple approach, each one of Eq. (11 and 12) will be utilized at the required thickness.

At the neutral line of the entire sandwich beam, via substituting $y = 0$ in Eq. (12), the bending stress will have zero value.

Combined stresses: This section serves as a solution, which provides a general means for establishing the normal and shear stresses components at a certain point on the sandwich beam's cross-section, which is

subjected to varied types of stresses occur simultaneously. To achieve this solution, the analysis that has been developed in the previous sections for the bending and transverse shear stresses will be utilized here.

The resultant stresses can be obtained as a maximum and minimum normal stresses and maximum shear stress for combined bending and shear stresses occurred due to concentrated load or distributed load presented in this research via using the following Mohr's circle dimensions or principal stresses and maximum in-plane shear stress relations in Eq. (13) from Khurmi and Gupta (2005):

$$\sigma_{1,2} = \frac{\sigma_x + \sigma_y}{2} \pm \sqrt{\left(\frac{\sigma_x - \sigma_y}{2}\right)^2 + \tau_{xy}^2}, \quad (13)$$

$$\tau_{max} = R = \sqrt{\left(\frac{\sigma_x - \sigma_y}{2}\right)^2 + \tau_{xy}^2},$$

$$\sigma_{avg} = \frac{\sigma_x + \sigma_y}{2},$$

$$C = (\sigma_{avg}, 0).$$

Static deflections: Always, boundaries must be placed on the amount of static deflection a sandwich beam or a solid beam undergoes when it is subjected to a load. Several calculations of static deflections were covered in this section under various types of loads. Where the main focuses of interest in this research are maximum

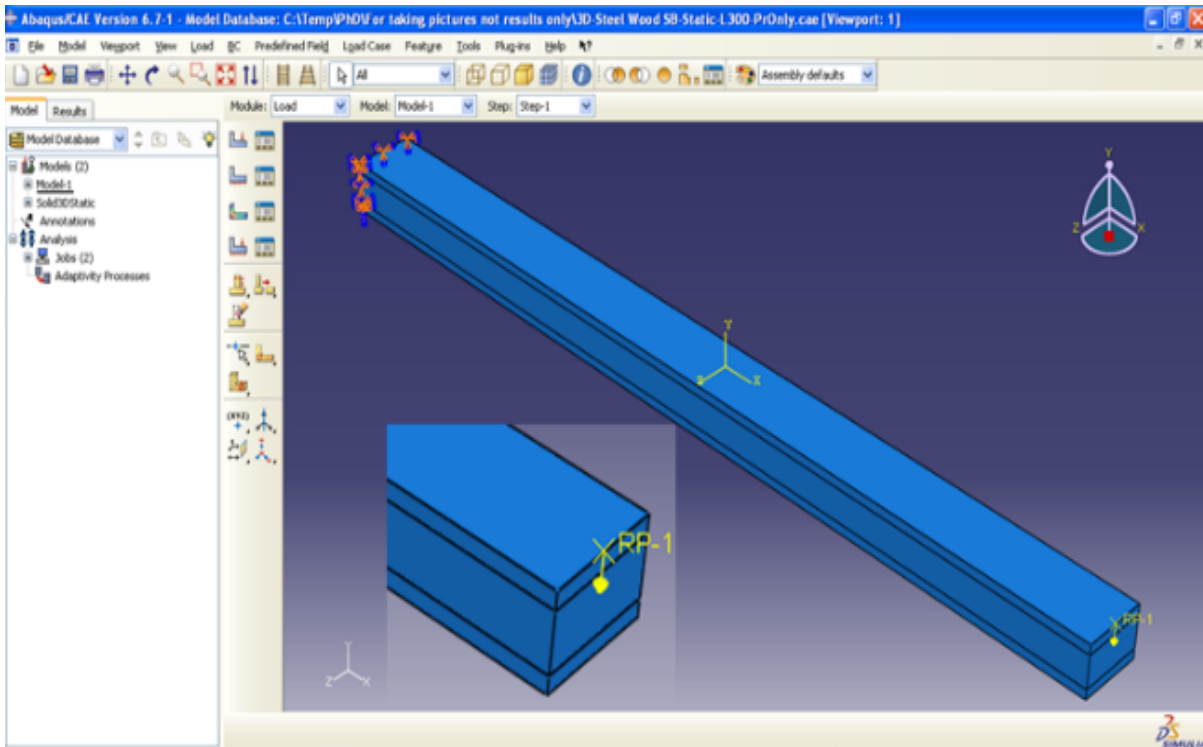


Fig. 4: Abaqus software presents a sandwich beam in cantilever geometry before applying a concentrated load

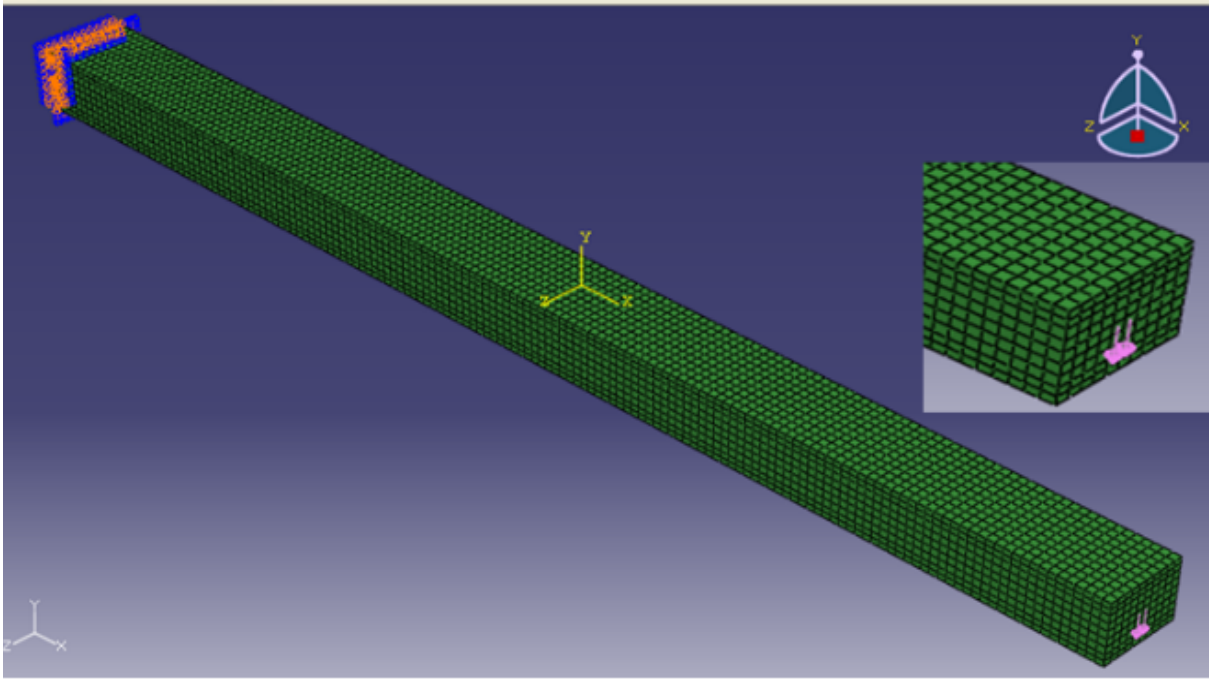


Fig. 5: Meshed sandwich beam as a cantilever before applying the shear force of 1.5 kN over its cross section

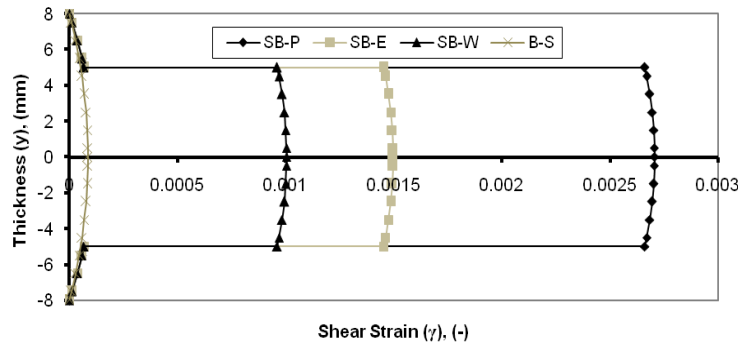


Fig. 6: Transverse shear strain of beam versus three sandwich beams with a different core material

deflections of cantilever sandwich beam due to a uniform distributed load w applied perpendicular on the longitudinal direction along the specimen or a concentrated load F applied perpendicular on the free end. Based on the linear superposition technique and with taken into consideration only the shear effect from the core material, because the face sheets effect on the static deflection value is small enough so that it can be neglected. The total static deflection of sandwich beam structure will have two contributor values caused by the bending and shear deformations, which can achievable via utilization of the flexural and shear rigidities as shown in Eq. (14):

$$Y = \frac{FL^3}{3D} + \frac{FL}{S}, \text{ and } Y = \frac{wL^4}{8D} + \frac{wL^2}{2S}. \quad (14)$$

Where: $S = \bar{k} * (GA)_c$,

and $\bar{k} = (5/6)$ for rectangular cross-section.

SIMULATION ANALYSIS

As presented in Fig. 4, Abaqus 6.7-1 was the commercial software used by the authors for applying their vision to obtain the targeted numerical results and simulation figures. With vision's commitment to compare these numerical simulation outputs alongside their equivalent theoretical results to achieve an acceptable matching for verifications purposes of present work conclusions.

A shear force will be dedicated to studying its shear stress effect on this research's specimens that always fixed as cantilever geometry as Fig. 5. Besides, there are two different classifications of the interested combined bending and shear stresses according to the type of load. These types of load are concentrated load F and distributed load w as presented in Fig. 4 and 9, respectively. Also, the principal stresses relations can

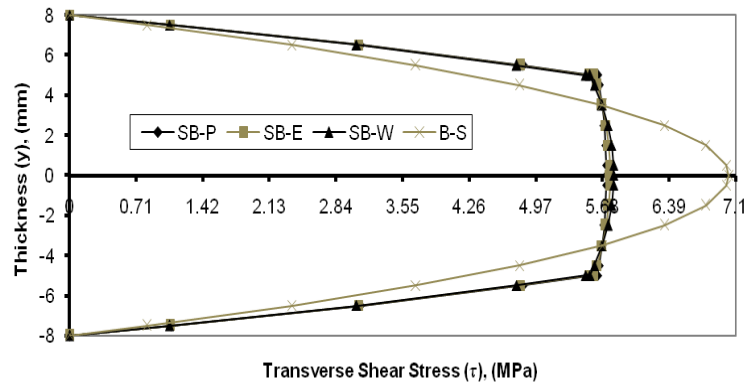


Fig. 7: Transverse shear stress of beam versus three sandwich beams with a different core material

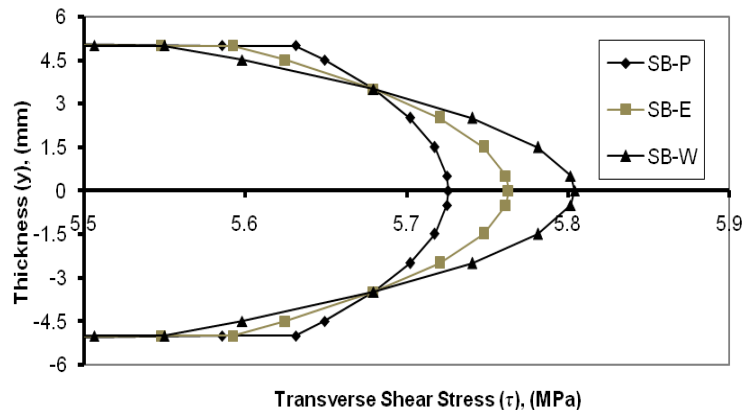


Fig. 8: Specific transverse shear stress for the core zone of three sandwich beams with a different core material

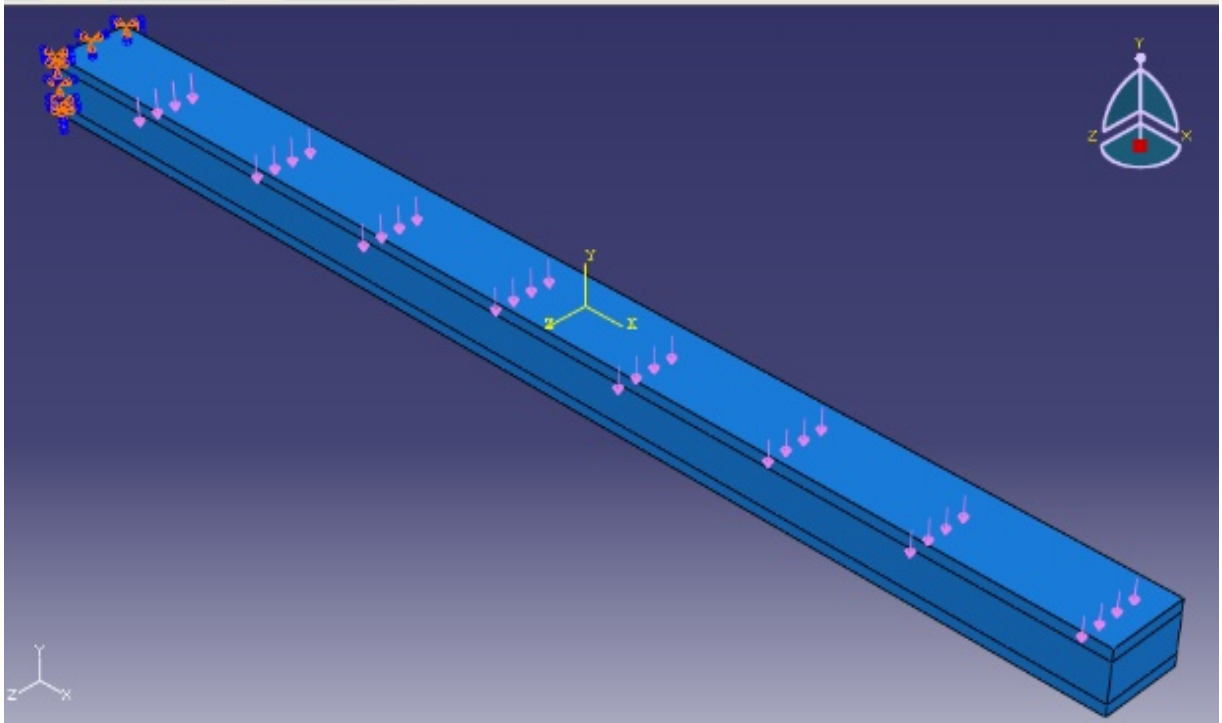


Fig. 9: Distributed load to be applied perpendicular on the longitudinal direction along the sandwich beam

Table 1: Mechanical specifications of solid beam and sandwich beam components

Component	Material	Modulus of elasticity (E), (GPa)	Modulus of rigidity* (G), (GPa)	Density (ρ), (kg/m ³)
Core	Polyamide	5.5	2.115	1300
	Epoxy	10	3.845	1400
	Wood	15	5.77	720
Face sheets	Steel 1020	210	80.77	7900

* Modulus of rigidity values are related to the modulus of elasticity values via $E = 2G(1 + 0.3)$

Table 2: Maximum shear strain values at the neutral line of the entire specimen

Specimen	SB-P	SB-E	SB-W	B-S
Shear strain (γ), (-)	0.270681E-2	0.149846E-2	0.100606E-2	0.008702E-2

Table 3: Maximum shear stress values at the neutral line of the entire specimen

Specimen	SB-P	SB-E	SB-W	B-S
Shear stress (τ), (MPa)	5.72593	5.76329	5.80421	7.02821

be utilized here because it is a good method to solve the problem of variance between bending and shear stresses within obtaining the resultant stresses.

For the utilized components of the solid beam and sandwich beams with different core material within this study, their mechanical specifications can be outlined in Table 1 from Abdel Salam and Bondok (2008).

Transverse shear stress: A shear force V equals 1.5 kN applied over the cross section of cantilever sandwich beam in a meshed state as shown in Fig. 5. While the shear strain, shear stress and specific shear stress for core zone were illustrated through Fig. 6 to 8 respectively.

From Fig. 6, the maximum values of shear strain for the various specimens can be achieved from the natural line of the entire structure and then outlined in Table 2.

Figure 7 presents the differences in the overall parabola forms of the transverse shear stress of a solid beam versus a sandwich one. While Fig. 8 presents the variation of transverse shear stress for a specific core zone of three sandwich beams with a different core material.

From Fig. 7, the maximum values of transverse shear stress for the various specimens can be achieved

from the neutral line of the entire specimen and then can be outlined in Table 3.

Combined stresses due to distributed load: A distributed load w equals 5 N/mm applied perpendicularly on the longitudinal direction along the cantilever sandwich beam as shown in Fig. 9 and then leading to cause combined bending and shear stresses, besides a static deflection. Therefore, the shear strain and stress were presented previously through Fig. 6 to 8, while the bending strain, bending stress, specific bending stress for the core zone; and downward deflection were illustrated through Fig. 10 to 13, respectively.

From Fig. 10 due to distributed load; the maximum values of bending strain for the various specimens can be achieved at fixation edge from the outer surface of the upper face and then outlined in Table 4.

Figure 11 demonstrates the consequences of a distributed load on the overall forms (straight and broken lines) of bending stress of solid beam versus a sandwich one. While Fig. 12 demonstrates the effect of distributed load on bending stress of a specific core zone of three sandwich beams with a different core material.

From Fig. 11 due to distributed load; the maximum values of bending stress for the various specimens can

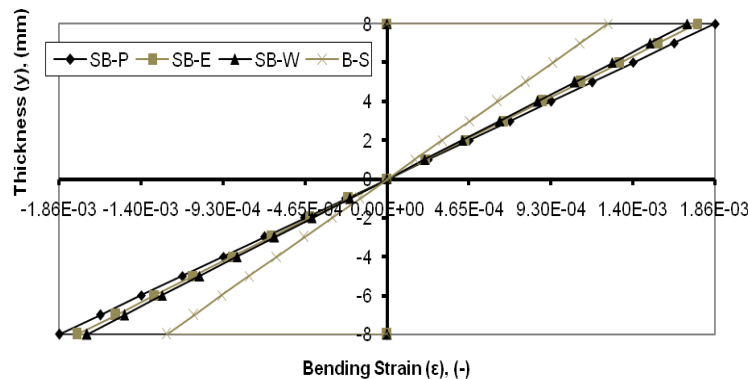


Fig. 10: Bending strain of beam versus three sandwich beams with different core material at fixation edge due to distributed load

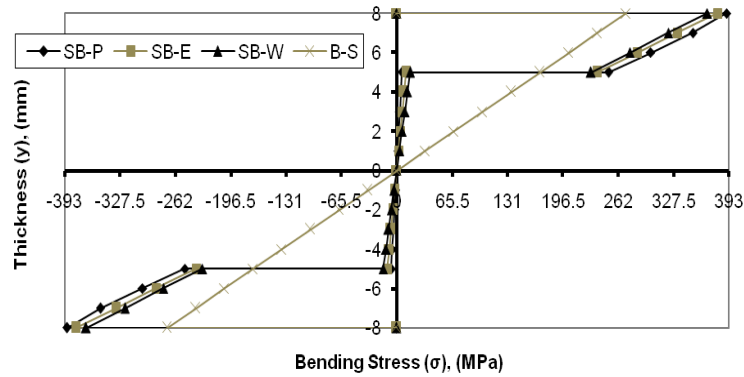


Fig. 11: Bending stress of beam versus three sandwich beams with a different core material (straight and zig-zag lines) at fixation edge due to distributed load

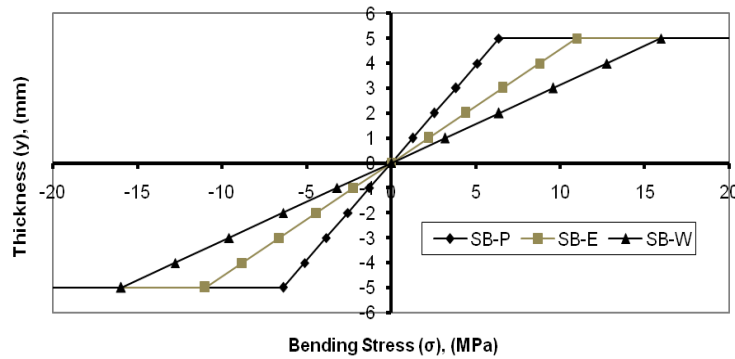


Fig. 12: Specific bending stress for the core zone of three sandwich beams with different core material at fixation edge due to distributed load

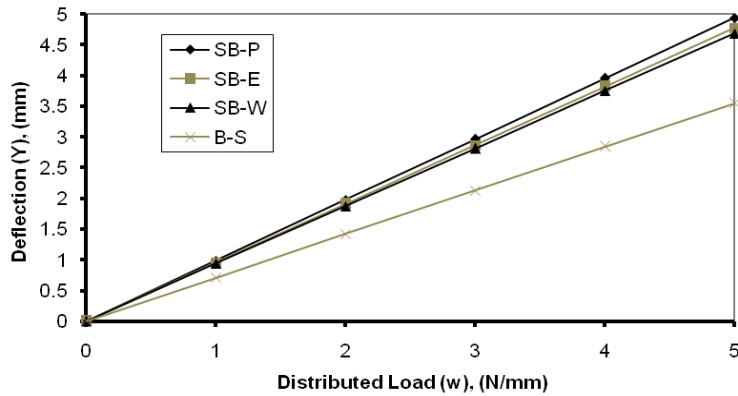


Fig. 13: Deflection of beam versus three sandwich beams with different core material due to a distributed load applied perpendicular on the longitudinal direction along the cantilever specimen

Table 4: Maximum values of bending strain at thickness 8 mm on the upper face at fixation edge due to distributed load

Specimen	SB-P	SB-E	SB-W	B-S
Bending strain (ϵ), (-)	0.185872E-2	0.175796E-2	0.170181E-2	0.125116E-2

Table 5: Maximum values of bending stress at thickness 8 mm on the upper face at fixation edge due to distributed load

Specimen	SB-P	SB-E	SB-W	B-S
Bending stress (σ), (MPa)	390.331	379.731	367.832	271.874

be achieved at fixation edge from the outer surface of the upper face and then outlined in Table 5.

Due to distributed load; the resultant stresses of combined bending and shear ones can be achieved as a

Table 6: Resultant stresses of combined bending and shear ones at the outer surface of the upper face at fixation edge due to distributed load

Specimen	SB-P	SB-E	SB-W	B-S
Maximum normal stress (σ_{max}), (MPa)	390.331	379.731	367.832	271.874
Minimum normal stress (σ_{min}), (MPa)	0	0	0	0
Maximum In-Plane shear stress (τ_{max}), (MPa)	195.166	189.866	183.916	135.937

Table 7: Values of deflection of beam versus three sandwich beams with different core material due to distributed load 5 N/mm

Specimen	SB-P	SB-E	SB-W	B-S
Deflection (Y), (mm)	4.93899	4.7757	4.68699	3.55242

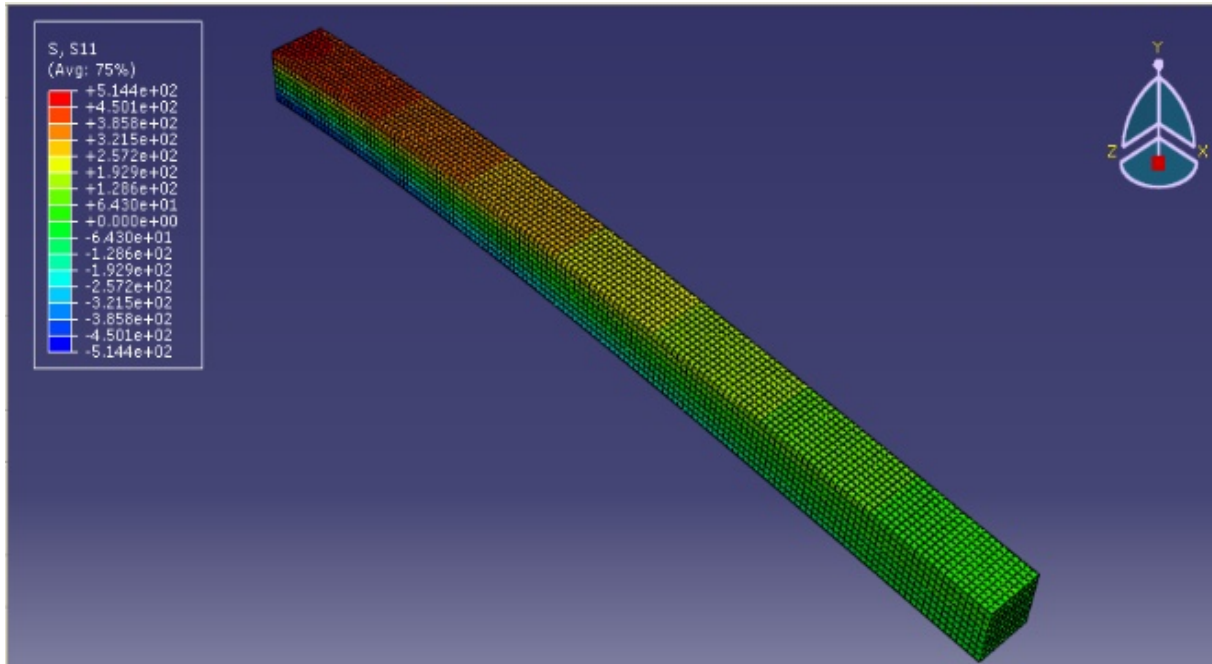


Fig. 14: Bended (B-S) specimen after applying a concentrated load of 1.5 kN

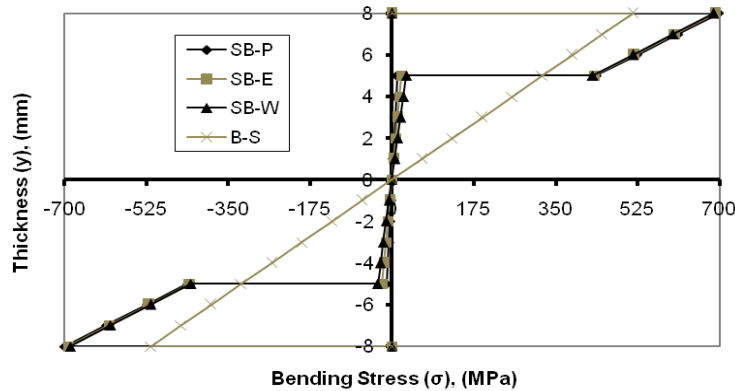


Fig. 15: Bending stress of beam versus three sandwich beams with a different core material (straight and zig-zag lines) at fixation edge due to concentrated load

maximum and minimum normal stresses and maximum in-plane shear stress as presented in Table 6.

Beside from Fig. 13, the static values of downward deflection as an outcome for the distributed load can be achieved and outlined in Table 7.

Combined stresses due to concentrated load: A concentrated load F equals 1.5 kN applied

perpendicular on the free end of cantilever specimen. Therefore, the resultant bent specimen from Abaqus software was demonstrated in Fig. 14. As consequences, the shear strain and stress were demonstrated previously through Fig. 6 to 8, while the bending stress and downward deflection were illustrated in Fig. 15 and 16, respectively.

Table 8: Maximum values of bending stress at thickness 8 mm on the upper face at fixation edge due to concentrated load

Specimen	SB-P	SB-E	SB-W	B-S
Bending stress (σ), (MPa)	698.716	691.512	687.246	514.818

Table 9: Resultant stresses of combined bending and shear ones at the outer surface of the upper face at fixation edge due to concentrated load

Specimen	SB-P	SB-E	SB-W	B-S
Maximum normal stress (σ_{max}), (MPa)	698.716	691.512	687.246	514.818
Minimum normal stress (σ_{min}), (MPa)	0	0	0	0
Maximum In-Plane shear stress (τ_{max}), (MPa)	349.358	345.756	343.623	257.409

Table 10: Values of deflection of beam versus three sandwich beams with different core material due to concentrated load 1.5 kN

Specimen	SB-P	SB-E	SB-W	B-S
Deflection (Y), (mm)	12.9982	12.6397	12.4351	9.47056

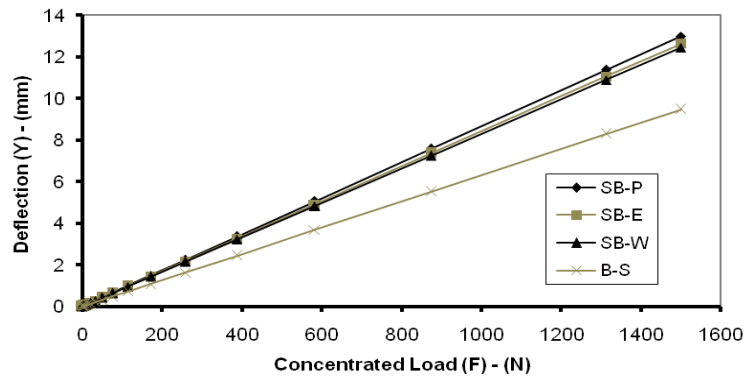


Fig. 16: Deflection of beam versus three sandwich beams with different core material due to a concentrated load applied perpendicular on the free end of cantilever specimen

From Fig. 14 and 15 which demonstrates the variance in overall forms (straight and broken lines) of bending stress under a concentrated load of solid beam versus a sandwich one; the maximum values of bending stress for the various specimens can be achieved at fixation edge from the outer surface of the upper face and then outlined in Table 8.

Due to concentrated load, the resultant stresses of combined bending and shear ones can be achieved as a maximum and minimum normal stresses and maximum in-plane shear stress as presented in Table 9.

Beside from Fig. 16, the static values of downward deflection as an outcome for the concentrated load can be achieved and outlined in Table 10.

RESULTS AND DISCUSSION

First, to validate the present theoretical and simulation results with each other, comparisons have been performed and presented in shear, distributed load and concentrated load studies. Second, for the correlation and validation between the present results and results published in Dai and Zhang (2008) plus other works, comparisons of concepts have been executed and displayed through Fig. 17 to 19.

Although, both present and mentioned published results produced from researches study the same concepts of shear stress, bending stress and static deflection; there are some variations should be taken

into consideration to understand the very acceptable comparison between them. First, the dimensions of the specimens and the effective loads have different values. Second in Fig. 17 and 18, vertical and horizontal axes reversed with each other between the current study and Dai and Zhang (2008) work.

As shown in Fig. 17, the overall parabola shape of shear stress and the location of maximum shear stress of sandwich structures, which exists at the neutral line, were displayed in a good matching pattern in both Fig. 17a and 17b, which leads to exhibit good support.

Also, a good correlation between our results and Carrera (2003) work from the point of view of the continuity of the shear stress diagram especially at each layer interface based on the broken line theory (zig-zag theory).

As displays in Fig. 18, the general broken-line (zig-zag) shape of the bending stress of sandwich beam, which constructed from combinations of bending stresses of both core and face sheets, is displayed in a good matching pattern in both Fig. 18a and 18b, which leads to exhibit good support.

Also, a good correlation between our results and Sayyad and Ghugal (2017) work from the point of view of finite element modeling and bending stress, where the broken-line theory (zig-zag theory) was observed in our results of bending diagrams.

As present in both Fig. 19a and 19b, an inverse relationship between the flexural rigidity D and the

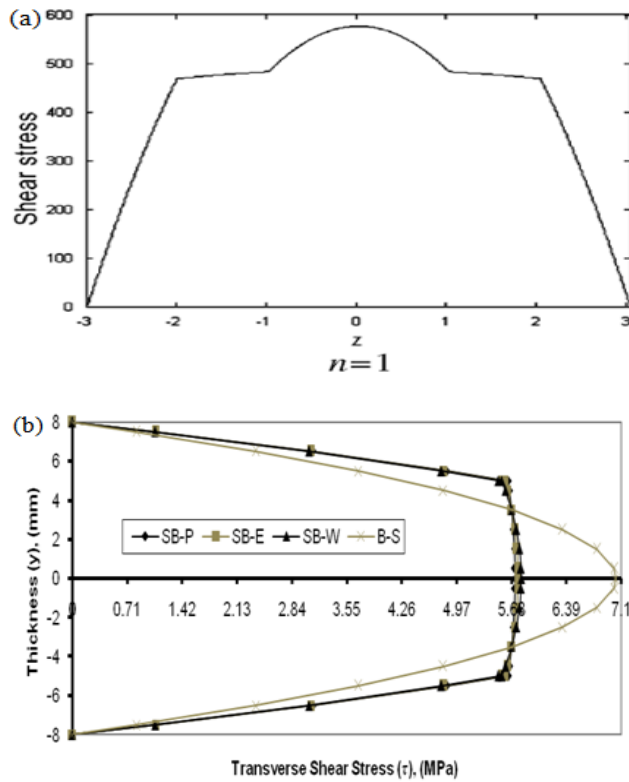


Fig. 17: Shear stress allocation: (a) from Dai and Zhang (2008), here, z is the thickness direction and n is the cells number (one cell contains two faces and one core) and (b) from present work

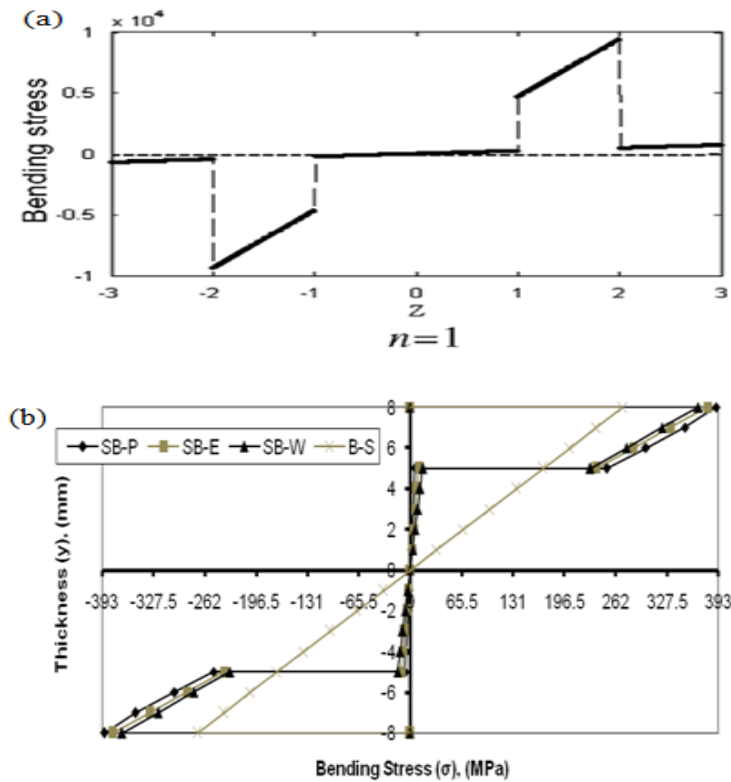


Fig. 18: Bending stress allocation: (a) from Dai and Zhang (2008) and (b) from present work

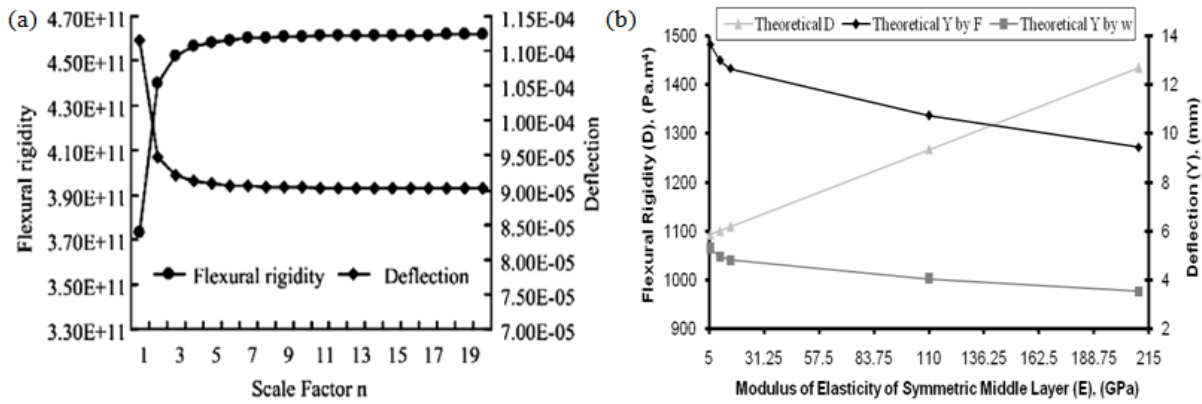


Fig. 19: The relationship between static deflection and flexural rigidity: (a) from Dai and Zhang (2008) and (b) from present work

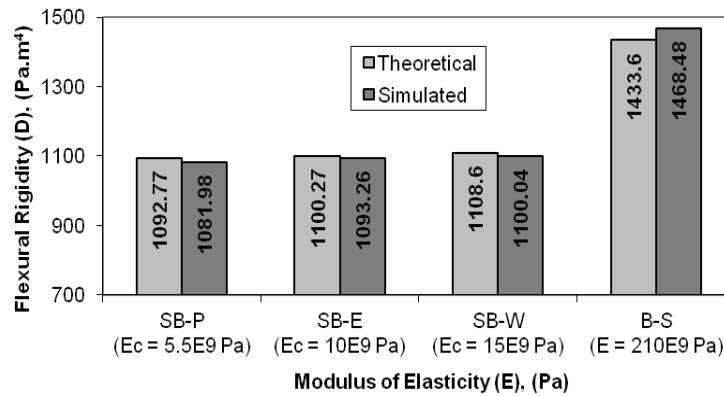


Fig. 20: Effect of sandwich beams with different core material versus solid beam on the overall flexural rigidity

Table 11: Comparison between theoretical and simulation results of a shear study at specimen’s neutral line

Specimen	Flexural Rigidity D, Pa.m ⁴		Shear stress τ , MPa		Shear strain γ , -	
	Theoretical	Simulation	Theoretical	Simulation	Theoretical	Simulation
SB-P	1092.77	1081.98	5.71542	5.72593	0.270233E-2	0.270681E-2
SB-E	1100.27	1093.26	5.75315	5.76329	0.149627E-2	0.149846E-2
SB-W	1108.6	1100.04	5.79447	5.80421	0.100424E-2	0.100606E-2
B-S	1433.6	1468.48	7.03125	7.02821	0.008705E-2	0.008702E-2

static deflection Y is displayed in good support, where increasing D leads to decrease Y and vice versa.

Shear study: The influence of utilizing sandwich beam instead of a solid one, on the stress analysis of restricted shear force over the cross-section of cantilever specimen, is discussed through demonstration of flexural rigidity, shear strain and shear stress in Table 11, Fig. 20 and 21.

The results of the shear study in comparison Table 11, Fig. 20 and 21 display good matching by about (97.5%) between theoretical and simulated outputs.

As a first result as presented in Fig. 20, employment sandwich beam with the lowest core modulus of elasticity instead of a solid beam leads to decrease of core flexural rigidity due to the incremental relationship between them (E_c and D_{co}) as mentioned in

Eq. (3) and hence moderately decrease the specimen’s overall flexural rigidity.

As a second result as presented in Fig. 21, employment sandwich beam with the lowest core modulus of elasticity instead of a solid beam; moderately decreases shear stress at the neutral line due to multiply the core modulus of elasticity by the core thickness square as proved in Eq. (9), on contrast and very significantly increases the shear strain at the neutral line due to a low value of core shear modulus which draws from lower flexural rigidity of sandwich beam compared to a solid one.

Distributed load study: The influence of utilizing sandwich beam instead of a solid one, on the stress analysis of distributed load restricted perpendicularly on the longitudinal direction along the cantilever

Table 12: Comparison between theoretical and simulation results of distributed load study on the face's outer surface and core's highest thickness at fixation edge

Specimen according to rigidity D , Pa.m^4	Face bending stress σ_{Bf} , Mpa		Core bending stress σ_{Bc} , Mpa		Static deflection Y , mm	
	Theoretical	Simulation	Theoretical	Simulation	Theoretical	Simulation
SB-P ($D = 1092.77$)	345.911	390.331	5.66223	6.38935	5.27103	4.93899
SB-E ($D = 1100.27$)	343.553	379.731	10.2248	10.9873	4.95226	4.7757
SB-W ($D = 1108.6$)	340.971	367.832	15.2219	15.9545	4.80054	4.68699
B-S ($D = 1433.6$)	263.672	271.874	164.795	169.921	3.53132	3.55242

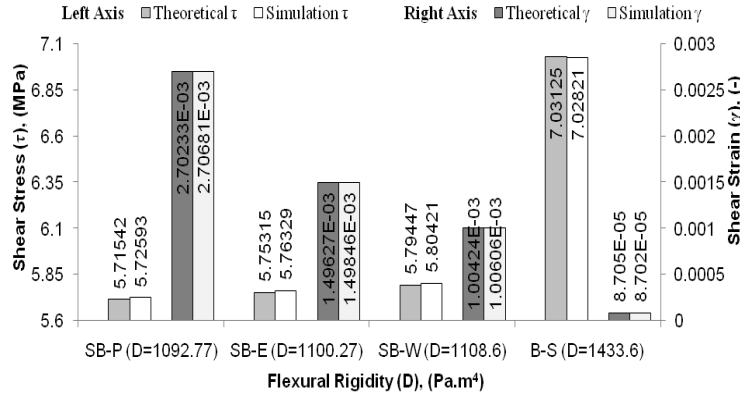


Fig. 21: Effect of sandwich beams with different core material versus solid beam on maximum results of shear stress and strain at the neutral line of the entire specimen

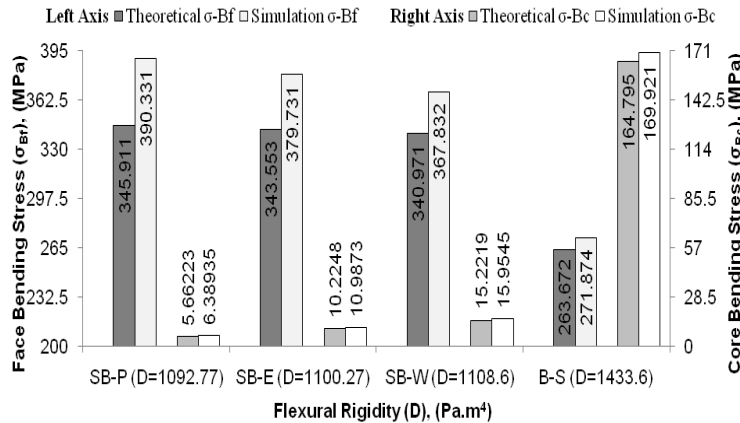


Fig. 22: Effect of sandwich beams with different core material versus solid beam on maximum results of bending stress at ($y = 5$ and 8 mm) at fixation edge due to distributed load

specimen, is discussed through demonstration of shear stress and strain in Fig. 21, flexural rigidity, bending stress at thicknesses (-8 to -5 and 5 to 8 mm) and thickness (-5 to 5 mm) of solid beam and sandwich beam where can be labeled as faces bending stress and core bending stress respectively for simplification and comparability purposes, maximum in-plane shear stress and static deflection in Table 12, Fig. 22 and 23.

The results of the distributed load study in comparison Table 12, Fig. 22 and 23 display good matching by about (87%) between theoretical and simulated outputs at fixation end. As results of employment sandwich beam with the lowest core modulus of elasticity instead of a solid beam; first one moderately increases the faces bending stress and strain, on contrast the second one, decreases the core

bending stress and strain significantly and moderately, respectively. Third, moderately increases the maximum normal stress and in-plane shear stress and fourth moderately increases the static deflection at the free end.

Here, the important leading role of the flexural rigidity will become clear, where the previous results were due to lower flexural rigidity D of the sandwich beam compared to a solid beam made from one material and beside of the incremental relationship between the core bending stress σ_{Bc} and the core modulus of elasticity E_c as mentioned in Eq. (12).

Concentrated load study: The influence of utilizing a sandwich beam instead of a solid one on the stress analysis of concentrated load restricted perpendicularly

Table 13: Comparison between theoretical and simulation results of concentrated load study on the face's outer surface at free and fixation edges

Specimen	Flexural rigidity D , Pa.m ⁴		Core bending stress σ , MPa		Static deflection Y , mm	
	Theoretical	Simulation	Theoretical	Simulation	Theoretical	Simulation
SB-P	1092.77	1081.98	691.822	698.716	13.6306	12.9982
SB-E	1100.27	1093.26	687.1062	691.512	12.9719	12.6397
SB-W	1108.6	1100.04	681.941	687.246	12.6455	12.4351
B-S	1433.6	1468.48	527.344	514.818	9.41685	9.47056

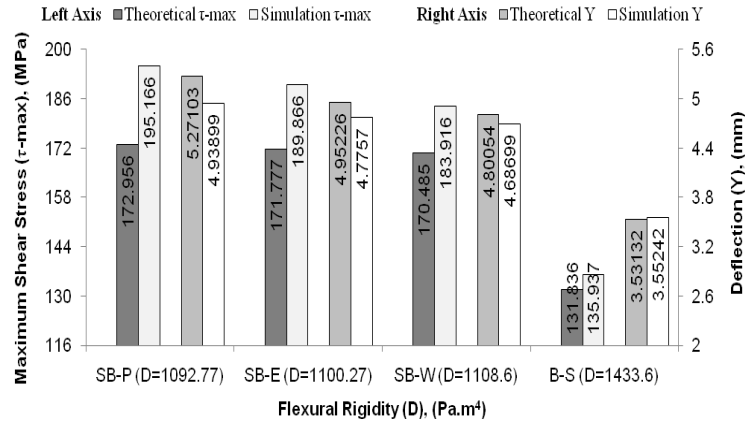


Fig. 23: Effect of sandwich beams with different core material versus solid beam within applied distributed load on maximum in-plane shear stress at fixation edge and static deflection at a free end

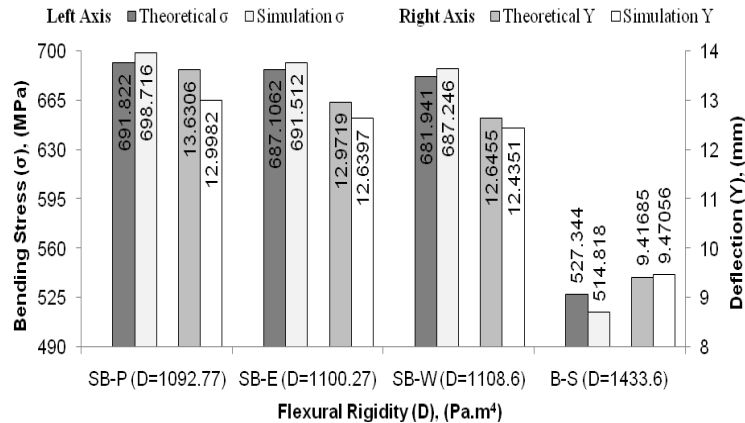


Fig. 24: Effect of sandwich beams with different core material versus solid beam within applied concentrated load on bending stress at fixation edge and static deflection at a free end

on the free end of cantilever specimen is discussed through demonstration of shear stress and strain in Fig. 21, flexural rigidity, static deflection and bending stress in Table 13 and Fig. 24. As well, using the simplification procedures and other comparison elements mentioned in distributed load study due to some degree of similarity between the two loadings studies.

The results of a concentrated load study in comparison Fig. 24 and Table 13 display good matching by about (95%) between theoretical and simulated outputs. As results, employment sandwich beam with the lowest core modulus of elasticity instead of a solid beam; moderately increases the faces bending stress and strain, also moderately increases the static

deflection at the free end and beside the other results from distributed load study.

The obtained results were due to lower flexural rigidity D of the sandwich beam compared to a solid beam made from one material.

CONCLUSION

Nowadays, the main design requirements that have a large scale of spreading in varied types of applications such as sustainable energy, constructions work, transportation industry, products manufacturing, communication instruments and fluid containing are high vibration damping and high rigidity to weight ratio.

Therefore, the main answer of the current work to the applications needs is introducing utilization of steel polyamide Sandwich Beam (SB-P) with low core modulus of elasticity instead of a solid steel Beam (B-S) having the same dimensions, in other words, via moderately decreasing the weight by about 50% and also means moderately decreasing the flexural rigidity by about 24%.

Further, after study and analysis this approach in cantilever geometry under shear force applied over the specimen's cross-section, a distributed load applied perpendicularly on the longitudinal direction along the specimen and a concentrated load applied perpendicularly on the specimen's free end; it can be concluded that:

The highest value of shear stress at the neutral line is moderately decreasing by about 19%, on contrast; the shear strain is very significantly increased by about 3000% and vice versa with the same overall trend.

In case of distributed load and at fixation edge position; the faces bending stress and strain are moderately increasing by about 30%, on contrast, the core bending stress is significantly decreasing by about 96% and the core bending strain is moderately decreasing, by the same percentage as the face strain increasing due to the same slope, by about 30%. Also, this swapping leads to moderately increase the

maximum normal and in-plane shear stresses, by the same percentage as the face stress increasing, by about 30%. Besides, the static deflection is moderately increasing by about 50% and vice versa with the same overall trend for all pre.

The observation case of a concentrated load at the specimen's free end and the stress at fixation edge position, with having the previously mentioned values of concentrated load, distributed load and the fixed value of specimen's length parameter, was useful. Where, the exchange between (SB-P) and (B-S) leads to moderately increase the faces bending stress and strain by about 30%, as well as, the same mentioned conclusions of the distributed load case will be applied due to some degree of similarity between the two load types. But, the static deflection at the free end is moderately increasing by about 45% and vice versa with the same overall trend for all pre.

The results were verified theoretically, numerically and with published work, however, the study sheds light towards more complex sandwich beam configurations and the dynamic performance variation between the sandwich and solid structures, but high vibration damping is an important requirement in the market applications; therefore, this will be the future concern of the next research.

Nomenclature:

A	Cross-sectional area of the sandwich beam (m ²)	V	Shear force (N)
A'	Top portion of the specimen's cross-sectional area, defined from the section where shear is measured (m ²)	w	Distributed load (N/m)
B	Width of the sandwich beam (m)	x	Longitudinal axis, Coordinates in the longitudinal direction, (m)
C	Center of Mohr's circle (m)	Y	Static deflection on the free end of cantilever specimen, (m)
c	Neutral line offset from the specimen's centroidal line (m)	y	Axis of symmetric, Coordinates in the thickness direction of a specimen (m)
D	Flexural rigidity or bending stiffness (Pa.m ⁴)	z	Coordinates on an axis perpendicular to the axis of symmetry (m)
D_{co}	Flexural rigidity of a core about its own neutral line and also about the neutral line of the entire sandwich beam (Pa.m ⁴)	γ	Shear strain (-)
D_f	Flexural rigidity of each face sheet about its own neutral line (Pa.m ⁴)	γ_{Bc}	Shear strain of a core material (-)
D_{fn}	Flexural rigidity of the face sheets about the neutral line of the entire sandwich beam (Pa.m ⁴)	γ_{Bf}	Shear strain of a face sheet (-)
d	Distance between the neutral lines of symmetric top and bottom layers (m)	ϵ	Strain (-)
E_i, E_l	Modulus of elasticity of a specific layer (GPa)	ϵ_{Bc}	Bending strain of a core material (-)
E_c	Modulus of elasticity of the core (GPa)	ϵ_{Bf}	Bending strain of a face sheet (-)
E_{eq}	Equivalent modulus of elasticity of the entire sandwich beam (GPa)	ρ	Density of a material (kg/m ³)
E_{lf}, E_{uf}	Modulus of elasticity of the face sheet, lower face, upper face respectively (GPa)	ρ_c	Density of the core material (kg/m ³)
F	Concentrated load (N)	ρ_f	Density of the face sheets material (kg/m ³)
G	Shear modulus (GPa)	σ_1, σ_2	Principal stresses as maximum and minimum normal stresses at a point (MPa)
G_c	Shear modulus of the core (GPa)	σ	Stress (MPa)
G_f	Shear modulus of the face sheet (GPa)	σ_{avg}	Average normal stress (MPa)
H	Total thickness of the sandwich beam (m)	σ_{Bc}	Bending stress of a core material (MPa)
h_f, h_{lf}, h_{uf}	Thickness of the face sheet, lower face, upper face respectively (m)	σ_{Bf}	Bending stress of a face sheet (MPa)
h_c	Thickness of the core (m)	σ_x, σ_y	Normal stress components (MPa)
I	Area moment of inertia of the sandwich beam (m ⁴)	τ	Shear stress (MPa)

Nomenclature: Continue

\bar{k}	Shear coefficient of the specimen with a rectangular cross-section (-)	τ_c	Shear stress of a core material (MPa)
L	Length of the sandwich beam (m)	τ_f	Shear stress of a face sheet (MPa)
M, M_b	Bending moment (N.m)	τ_{max}	Maximum shear stress at the neutral line of the entire specimen, Maximum in-plane shear stress (MPa)
m	Total mass of the sandwich beam (kg)	τ_{xy}	Shear stress component (MPa)
m_c	Mass of the core (kg)	(B-S)	Solid Beam of a Steel Material
m_f	Mass of the face sheets (kg)	(SB-E)	Sandwich Beam of Steel Epoxy
R	Radius of curvature, Radius of Mohr's circle (m)	(SB-P)	Sandwich Beam of Steel Polyamide
S	Shear rigidity (Pa.m ²)	(SB-W)	Sandwich Beam of Steel Wood

REFERENCES

- Abdel Salam, M. and N.E. Bondok, 2008. Theoretical and experimental investigations into the effect of the sandwich beam elements on its dynamic characteristics. *Ain Shams J. Mech. Eng.*, 2: 91-110.
- Abrate, S. and M. di Sciuva, 2017. Equivalent single layer theories for composite and sandwich structures: A review. *Composite Struct.*, 179: 482-494.
- Carrera, E., 2003. Historical review of Zig-Zag theories for multilayered plates and shells. *Appl. Mech. Rev.*, 56(3): 287-308.
- Dai, G.M. and W.H. Zhang, 2008. Size effect of basic cell in static analysis of sandwich beams. *Int. J. Solids Struct.*, 45(9): 2512-2533.
- Hayes, A.M., A.J. Wang, B.M. Dempsey and D.L. McDowell, 2004. Mechanics of linear cellular alloys. *Mech. Mater.*, 36(8): 691-713.
- Jing, L., X. Su, D. Chen, F. Yang and L. Zhao, 2019. Experimental and numerical study of sandwich beams with layered-gradient foam cores under low-velocity impact. *Thin-Walled Struct.*, 135: 227-244.
- Khurmi, R.S. and J.K. Gupta, 2005. *Machine Design*. 14th Edn., Eurasia Publishing House Ltd., Ram Nagar, New Delhi.
- Kim, J. and S.R. Sawanson, 2001. Design of sandwich structures for concentrated load. *Compos. Struct.*, 52(3-4): 365-373.
- Magnucka-Blandzi, E., 2011a. Dynamic stability and static stress state of a sandwich beam with a metal foam core using three modified Timoshenko hypotheses. *Mech. Adv. Mater. Struct.*, 18(2): 147-158.
- Magnucka-Blandzi, E., 2011b. Mathematical modelling of a rectangular sandwich plate with a metal foam core. *J. Theore. Appl. Mech.*, 49(2): 439-455.
- Manalo, A.C., T. Aravinthan and W. Karunasena, 2013. Shear behaviour of glued structural fibre composite sandwich beams. *Constr. Build. Mater.*, 47: 1317-1327.
- Noor, A.K., W.S. Burton and C.W. Bert, 1996. Computational models for sandwich panels and shells. *Appl. Mech. Rev.*, 49(3): 155-199.
- Reddy, J.N., 2010. Nonlocal nonlinear formulations for bending of classical and shear deformation theories of beams and plates. *Int. J. Eng. Sci.*, 48(11): 1507-1518.
- Reissner, E., 1944. On the theory of elastic plates. *J. Math. Phys.*, 23: 184-191.
- Romanoff, J. and P. Varsta, 2006. Bending response of web-core sandwich beams. *Compos. Struct.*, 73(04): 478-487.
- Sayyad, A.S. and Y.M. Ghugal, 2017. Bending, buckling and free vibration of laminated composite and sandwich beams: A critical review of literature. *Compos. Struct.*, 171: 486-504.
- Shehata, M.A.M., A.S.A. Abou-Taleb and A. Nassef, 2019. Investigation and simulation of mechanics of solid beam versus sandwich beams with different core material. *Res. J. Appl. Sci. Eng. Technol.*, accepted for publication.
- Steeves, C.A. and N.A. Fleck, 2004. Collapse mechanisms of sandwich beams with composite faces and a foam core, loaded in three-point bending. Part I: analytical models and minimum weight design. *Int. J. Mech. Sci.*, 46(4): 561-583.
- Wang, C.M., J.N. Reddy and K.H. Lee, 2000. *Shear Deformable Beams and Plates*. 1st Edn., Elsevier Science Ltd., Amsterdam, Lausanne, New York, Shannon, Singapore, Tokyo.